Heliyon 10 (2024) e37477

Contents lists available at ScienceDirect

Heliyon

journal homepage: www.cell.com/heliyon

Research article

Targeting ferroptosis promotes diabetic wound healing via Nrf2 activation

Tongcai Wang [a,b,c], Yin Zheng [d,e], Jun Zhang [d,e], Zhongming Wu [a,b,d,e,*]

[a] NHC Key Laboratory of Hormones and Development, Chu Hsien-I Memorial Hospital and Tianjin Institute of Endocrinology, Tianjin Medical University, Tianjin, 300134, China
[b] Tianjin Key Laboratory of Metabolic Diseases, Tianjin Medical University, Tianjin, 300134, China
[c] Department of Geriatric Medical Center, Inner Mongolia people's Hospital, 20 Zhaowuda Road, Hohhot, 010021, Inner Mongolia, China
[d] Key Laboratory of Endocrine Glucose & Lipids Metabolism and Brain Aging, Ministry of Education, Department of Endocrinology, Shandong Provincial Hospital Affiliated to Shandong First Medical University, Jinan, 250021, China
[e] Shandong Institute of Endocrine and Metabolic Diseases, Jinan, 250021, China

ARTICLE INFO

Keywords:
Ferroptosis
Diabetic wound healing
Ferrostatin-1
Anti-inflammation
Nuclear erythroid-associated factor 2

ABSTRACT

Wound healing impairment is a frequent diabetes problem leading to amputation. Hyperglycemia induces the overproduction of reactive oxygen species (ROS), iron overload and sustained inflammation, resulting in the persistence of chronic wounds. However, the intrinsic mechanisms of impaired diabetic wound healing remain enigmatic. A new non-apoptotic regulatory cellular death called Ferroptosis, is distinguished by iron-driven lipid peroxidation products accumulation along with insufficient antioxidant enzymes. A decline in antioxidant capacity, excess accumulation of peroxidation of iron and lipid have been identified in wound sites of streptozotocin-induced diabetes mellitus (DM) rats and elevated glucose (EG)-cultured macrophages. Additionally, sustained inflammation and increased inflammatory cytokines were observed in DM rats and HG-cultured macrophages. Importantly, ferrostatin-1 (Fer-1) is a ferroptosis suppressor treatment significantly ameliorated diabetes-related ferroptosis and inflammation. This treatment also enhanced cell proliferation and neovascularization, ultimately thereby accelerating diabetic wound healing. Meanwhile, our study demonstrated that an anti-ferroptotic and anti-inflammatory effects of Fer-1 were mediated through stimulation of nuclear erythroid-associated factor 2 (Nrf2). The current study may provide a new rationale for diabetic wound healing.

1. Introduction

Diabetes mellitus (DM) is an insulin resistance syndrome that afflicts approximately 340 million individuals worldwide[1]. Wound healing impairment is a major problem of uncontrolled diabetes, with approximately 20% of patients with DM developing diabetic wounds[2]. The prevalence of delayed wound healing in diabetic patients has persistently increased as a result of inadequate preventive and effective control measures. This high incidence of delayed wound healing among diabetics contributes to a major social and economic burden, also negatively affecting the quality of life for affected individuals.

* Corresponding author. NHC Key Laboratory of Hormones and Development, Chu Hsien-I Memorial Hospital and Tianjin Institute of Endocrinology, Tianjin Medical University, Tianjin, 300134, China.
E-mail address: wuzhongming@sph.com.cn (Z. Wu).

https://doi.org/10.1016/j.heliyon.2024.e37477
Received 22 May 2024; Received in revised form 4 September 2024; Accepted 4 September 2024
Available online 5 September 2024

Chronic hyperglycemia in diabetics adversely affects iron metabolism pathways, leading to decreased utilization of circulating transferrin and ferritin iron binding sites. Consequently, this results in an accumulation of free plasma iron[3]. Conversely, a decrease in iron concentration, achieved through dietary iron restriction, iron chelation, or venotomy, has been demonstrated to enhance beta cell function indiabetic animal models[4]. Elevated iron levels facilitate the highly toxic radicals production, like hydroxides (OH^-) and superoxide anions ($O_2^{\bullet-}$), which induce lipid peroxidation via the Fenton reaction. Furthermore, an excess of iron in tissues exacerbates the detrimental effects of free radicals and promotes inflammation[5].

Impaired wound healing in diabetics correlates with elevated oxidative stress levels. Hyperglycemia exacerbates the intracellular ROS production, results in persistent oxidative stress and lipid peroxidation. This imbalance at the cellular level impedes the wound-healing trajectory [6]. In addition, in chronic diabetic wounds, excessive ROS production disequilibrates theredox homeostasis, leading to loss of antioxidant capacity and increasing susceptibility to oxidative stress[7]. Overproduction and unregulated oxidative stress also leads in the chronicity and inflammation dysregulation, causing the persistence of chronic wounds[8]. A non-apoptotic form of controlled cell death called Ferroptosis, is depicted by iron-dependent lipid peroxides accumulation, coupled with an insufficiency of antioxidant enzymes to counteract this buildup [9]. Ferroptosis mediates the pathophysiological effects of ROS and lipid peroxidation by-products, thereby disrupting wound healing caused by diabetes were postulated.

Nrf2 is a transcriptional factor situated in the nucleus that controls the production of antioxidants[10]. It has integral roles in various cellular processes; notably, its downstream targets significantly influence iron metabolism [11] and manage inflammatory responses[12]. In prior research, Nrf2 has been pinpointed as a pivotal regulator of iron metabolism-related factors, such as ferritin and ferroportin (FPN), by controlling their expression at the transcriptional level [13]. Consequently, we postulate that the activation of Nrf2 may suppress diabetes-associated ferroptosis and inflammation.

Ferrostatin-1 (Fer-1), a suppressor of recognized ferroptosis, that has been documented to decelerate diabetic nephropathy progression [3]. Additionally, it exhibits anti-inflammatory properties across various diseases psoriasis, cerebral hemorrhage, and osteoarthritis[14]. However, the effects of Fer-1 on diabetic wound healing remain enigmatic. Emerging literature intimates a plausible regulatory interaction between Fer-1 and the Nrf2 pathway. For instance, Fer-1 counteracts foam cell formation caused by increased uric acid, through Nrf2-mediated autophagy and regulation of ferroptosis[15]. Through the Nrf2 pathway, an analog of Fer-1, Srs11-92, alleviated oxidative stress in cerebral ischemia/reperfusion injury [16]. Similarly, Fer-1 reduced liver damage from sepsis, correlating with increased Nrf2 expression[17]. The pivotal part of Nrf2 in managing oxidative stress and inflammation were given, this study seeks to ascertain if Fer-1 enhances diabetic wound healing by inhibiting ferroptosis and inflammation through Nrf2 activation.

Based on the above research, we postulated that Fer-1 mitigates diabetes-related ferroptosis and inflammation by the upregulation of Nrf2 expression, thereby promoting diabetic wound healing. Consequently, we embarked on a comprehensive investigation of the pathogenic underpinnings of impaired diabetic wound healing associated with ferroptosis both *in vitro* and *in vivo*, revealing the basic mechanism involving Nrf2 activation. Our study provided a novel understanding into the underlying mechanism of diabetic wound healing by focusing on ferroptosis as a therapeutic target. Additionally, this study offers a fresh therapeutic strategy for addressing impaired wound healing caused by DM.

2. Materials and methods

2.1. Cell culture

In Dulbecco's Modified Eagle Media (DMEM, Gibco, Carlsbad,CA,USA) which consists of 10 % fetal bovine serum (FBS, Biological Industries, Cromwell, CT, USA), 5.5 mmol/L glucose, 100 U/mL of both streptomycin and penicillin (SolarBio, Beijing, China) RAW264.7 cells (Collection of American Type Culture, Rockville, Maryland, USA), which are murine macrophages, were cultured. At 37 °C, Cell cultures were maintained in a 5 % CO_2 air incubator. The conditions of Standard cell culture served as the control group (Ctrl group), while cells cultured in DMEM comprising of 33.3 mmol/L glucose for 48 h constituted the high glucose group.

2.2. Drug treatment

The following reagents were used to treat RAW264.7 cells at the specified concentrations: RSL-3 (500 nmol/L, HY-100218A, MedChemExpress), Fer-1 (1 μM, A4371, ABExBIO), 0.1 % dimethyl sulfoxide (DMSO, as a vehicle control), Mannitol (constituted by 5.5 mmol/L glucose + 27.8 mmol/L mannitol, Solarbio, Beijing, China). All chemicals used were of analytical grade and solutions were sterilized. Cells in the RSL-3 groupwere cultured in DMEM with 5.5 mmol/L glucose for 48 h, while cells in the Fer-1 group were incubated in DMEM with 33.3 mmol/L glucose for the same duration. Concentrations for drug treatment were based on previously reported[14].

2.3. Cell viability assay

Followed by manufacturer's protocol, using the Cell Counting Kit-8 (CCK-8; Dojindo, Kumamoto, Japan), viability of Cell was assessed. Cells were incorporated in a 96-well plate and subsequently added specified concentrations of Fer-1, DMSO, or RSL-3 for 24 h. Then, 10 μL of CCK-8 solution was incorporated into each well andincubated in a 37 °C incubator for 2 h. At 450 nm, the absorbance was measured with a microplate reader (Synergy HT, Bio-Tek, United States).

2.4. Transmission electron microscopy (TEM)

TEM was carried out based on the methodology described in a previous study [19]. Cultured cells were fixed in 2.5 % glutaraldehyde, dehydrated in a graded alcohol series, infiltrated with an acetone-epoxy resin blend, and sectioned into ultra-thin slices. Subsequently, using a TEM (HT7700-SS; Hitachi, Tokyo, Japan), using lead citrate and uranyl acetate stain, sections were examined.

2.5. Iron assay

To evaluate iron content in tissues and cells, using a vibrating homogenizer for tissues collected samples were homogenized and an ultrasonic cell disrupter for cellular samples to procure the supernatant. The Iron Assay kit (BioAssay, Hayward, CA, USA) was subsequently employed to quantify iron levels as per the manufacturer's guidelines. The provided working reagents were mixed with the collected supernatants and dispensed into a 96-well plate. At 590 nm, microplate reader (Synergy HT, Bio-Tek, United States) was used, the optical density (OD) was detected.

2.6. Detection of malondialdehyde (MDA) and glutathione (GSH)levels

Tissues and cells were homogenized as described above. After centrifugation of the homogenate, the supernatant was collected. MDA and GSH concentrations were ascertained using the MDA Assay Kit and GSH Assay Kit (Solarbio, Beijing, China), respectively.The OD for MDA were determined at wavelengths of 600, 532, and 450 nm, while the OD for the GSH assay was recorded at 412 nm.

2.7. Detection of total ROS

Total ROS production in cells was determined as outlined earlier [3,18]. For assessing intracellular ROS levels, 2′,7′-dichlorofluorescin diacetate (DCFDA, Solarbio, Beijing, China) was employed. Cells, cultivated on coverslips until approximately 60 % confluence, were treated with 10 μM DCFDA and at 37 °C it was incubated for 30 min in the dark. Post-incubation, the coverslips were then rinsed with phosphate-buffered saline (PBS). After rinsing, cells were fixed with 4 % paraformaldehyde and counterstained with 4′,6-diamidino-2-phenylindole (DAPI). After fixation, they were thrice rinsed with PBS. Next, an antifading mounting medium was applied to the cells, and the coverslip was positioned atop. With the help of Zeiss confocal laser scanning fluorescence microscope, the samples were then analyzed.

2.8. Establishment of DM rat model

Adult male Sprague Dawley rats (n = 24), weighing 250–300 g, were housed in polycarbonate cages under a controlled habitat with a 12-h light-dark cycle, maintained at a constant temperature of 25 °C and consistent humidity levels. All rats had unrestricted access to clean water and standard rat chow *ad libitum*. The rats were administered i.p. injections of streptozotocin (STZ, 50 mg/kg,dissolved in 0.1 M citrate buffer, Sigma, USA) following a one-week acclimatization period to induce diabetes [18,19]. Control rats were given equal intraperitoneal (i.p.) doses of citrate buffer.Rats that consistently exhibited a random blood glucose concentration greater than 16.7 mm/L for three consecutive days were added in the study. All the animal experiments have complied with the Tianjin Medical Experimental Animal Care guidelines and animal protocols were approved by the Institutional Animal Care and Use Committee of Yi Shengyuan Gene Technology (Tianjin) Co., Ltd. (protocol number YSY-DWLL-2022081) on January 2, 2022. The animal experiments followed the principles of the Declaration of Helsinki (DOH, 2013 version). Upon reaching their respective survival time points, rats were anesthetized, shaved, and sterilized. Two full-thickness circular incisions, each 2 cm in diameter, were inflicted on their dorsum. Rats were then stratified into four groups: 1) non-diabetic control (NC); 2) diabetic: untreated (DM); 3) Fer-1 treated (DM/Fer-1); 4) DMSO treated (DM/VEH). Fer-1 (2 μg/kg, in 0.01 % DMSO) and 0.01%DMSO were injected into the wound base of DM rats in DM/Fer-1 and DM/VEH groups, respectively.

2.9. Calculation of rate of wound healing

On the day 0, 3, 7, 10, and 14 of post-surgery, wounds from each rat group were digitally photographed. Wound healing areas were then quantified using ImageJ software (NIH, USA). The formula for calculation of the rate of wound healing is as follows: Rate of Wound Healing = $(S_0\text{-}S_A)/S_0 \times 100$ %, where S_0 indicates an initial wound area on day 0, and S_A denotes the wound area on day A [19,20].

2.10. Hematoxylin and eosin (H&E) and immunohistochemistry staining

On the 14th day, all rats were euthanized, and skin samples surrounding the wounds were collected from each group for further examination. These samples were submerged in a 4 % paraformaldehyde fixative for 24 h and subsequently incorporated in paraffin. Following this, the tissues were sectioned into 4 μm-thick slices, after which they were deparaffinized and subsequently rehydrated. H&E staining [21,22] was carried out to analyze tissue inflammation and pathological alterations. After deparaffinization and rehydration, for immunohistochemistry [21–23], H_2O_2 was added to the sections for 15 min to quench activity of endogenous peroxidase. Consequently, the sections were blocked with 5 % goat serum for 1 h to diminish non-specific binding. The sections were

then incubated with primary antibodies for up to 72 h at 4 °C. Primary antibodies were rabbit anti-rat CD31 (ab28364; Abcam, Cambridge, MA, USA), GPX4 (ab125066; Abcam, Cambridge, MA, USA), SLC7A11 (ab175186; Abcam, Cambridge, MA, USA), and TFR-1 (ab214039; Abcam, Cambridge, MA, USA). The sections were rinsed three times and incubated with respective secondary antibodies for 1 h. Diaminobenzidine (DAB) was applied for visualization, followed by hematoxylin counterstaining for nuclei

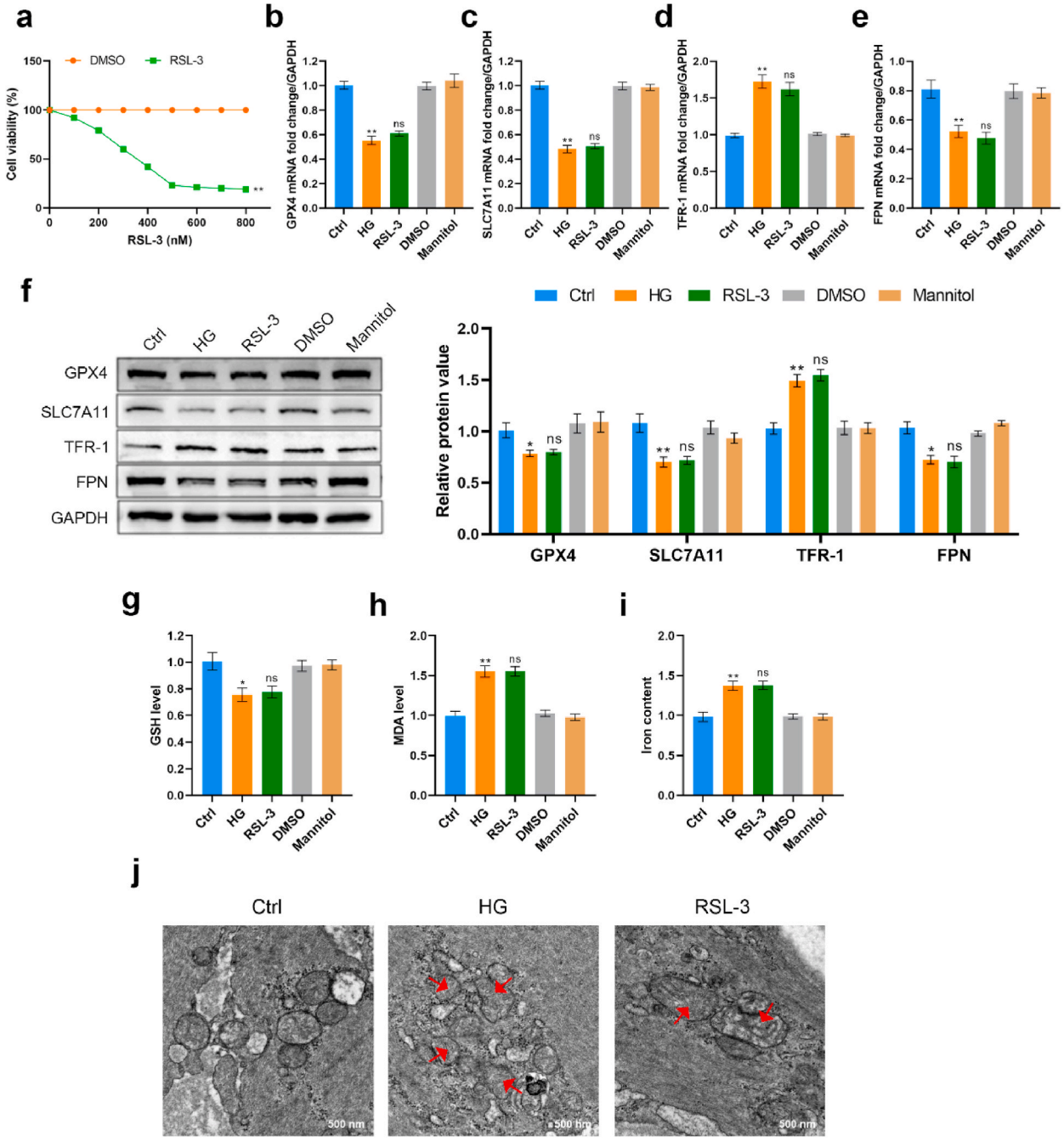

Fig. 1. Ferroptosis occurred in high glucose (HG)-cultured macrophages. (a) The viability of macrophage RAW264.7 cells was grown in 5.5 mmol/L DMEM, then exposed to rising concentrations of RSL-3 (0–800 nM) for 48 h **p < 0.01 vs. DMSO group. (b–e) The relative mRNA expression of ferroptosis-related indicatorsGPX4, SLC7A11, TFR-1, and FPN in RAW264.7 cells. (f) Theprotein expressionof GPX4, SLC7A11, TFR-1, and FPN in RAW264.7 cells. (g–i) The GSH, MDA, and iron content in RAW264.7 cells. (j) TEM images of mitochondrial structural changes in RAW264.7 cells. The red arrow shows mitochondria cristae disruption and outer mitochondria membrane rupture. (b–j) RAW264.7 cells were cultured with HG, RSL-3, DMSO, or mannitol. Values are expressed as mean ± standard deviation (SD). *p < 0.05, **p < 0.01 vs. Ctrl group; ns (not significant) vs. HG group. The uncropped and full-size images for (Fig. 1f) this figure are provided in Supplementary Fig. S1.

highlighting. Under a light microscope Samples were examined (Carl Zeiss Microscopy International, Germany) and resultant images were examined with ImageJ software (Madison, WI, USA). The relative expression of CD31, GPX4, SLC7A11, and TFR-1 was gauged by comparing the DAB staining density in the positive areas.

2.11. Immunofluorescent staining

For immunofluorescence staining, tissues were prepared as described above. After dewaxing, hydration, and blocking, sections were incubated with the primary antibody, Nrf2 (YT3189; Immunoway, Plano, TX, USA). DAPI was then applied as a counterstain to mark the cell nuclei. Using a fluorescence microscope (Olympus, Tokyo, Japan), sections were mounted and visualized.

2.12. Quantitative real-time PCR (qRT-PCR)

Overall RNA was isolated from skin tissue samples and RAW264.7 cells by the overall RNA extraction kit (Omega Bio-Tek, Norcross, GA, USA), adhering to the manufacturer's recommended protocols. A reversely transcription kit was employed to synthesize cDNA. Real-time PCR amplification was subsequently carried out by using specific primers and an SGExcel FastSYBR mixture, employing a qPCR system (Bio-Rad, Hercules, CA, USA). The change of fold was analyzed based on the $2^{-\Delta\Delta CT}$ method. Details of PCR primer sequences are presented in Supplementary Table S1.

2.13. Western blot analysis

Western blotting was performed as described elsewhere[23]. Rat tissue samples and RAW264.7 cells were lysed with RIPA buffer and proteins were isolated using SDS-PAGE before being transferred to PVDF membranes. Following this, the PVDF membranes were blocked in 5 % nonfat milk containing 0.1 % tris-buffered saline-tween-20 for 1 h to reduce non-specific binding. At 4 °C, the membranes were incubated overnight with the following primary antibodies: Nrf2 (YT3189; ImmunoWay, USA), GPX4 (ab125066; Abcam, USA),SLC7A11 (ab175186; Abcam), FPN (ab239583; Abcam, USA), TNF-α (ab183218; Abcam), TFR-1 (ab214039; Abcam), iNOS(#13120, Cell Signaling Technology, MA, USA), TGF-β (#3711, Cell Signaling Technology), Arg-1 (#89872, Cell Signaling Technology), and GAPDH (60004-1-Ig; Proteintech, Wuhan, China). Consequently, the membranes were probed with the appropriate secondary antibody for 1 h to visualize protein bands. Then, the membranes were subjected to enhanced chemiluminescence (ECL) solution to facilitate protein visualization and protein images were captured using a chemiluminescence instrument (Advansta, Menlo Park, CA).

2.14. Statistical analysis

Data in this study come from a minimum of three independent experiments to ensure consistency and validity. Results are displayed as mean ± standard deviation. By using One-way analysis of variance (ANOVA) compare multiple groups differences. The unpaired Student's t-test was carried out to examine variations among the two groups.$P < 0.05$ was taken as statistically significant.

3. Results

Ferroptosis is a distinct, iron-dependent type of non-apoptotic cell death, marked by increased lipid peroxidation, and is believed to play a pivotal role in the complications associated with wound healing caused by diabetes. The present study was conducted to explore the contribution of ferroptosis to wound healing caused by diabetes and to illustrate the associated mechanism, particularly focusing on the reactivation of Nrf2.

3.1. Ferroptosis occurred in HG-cultured macrophages

Macrophages are vital players in the process of wound-healing, as they are responsible for regulating inflammation, clearing cell debris and tissue repair coordination[24].Here, macrophage RAW264.7 cells were employed to investigate whether exposure to high glucose concentrations could induce ferroptosis *in vitro*. RSL-3 is a well-known ferroptosis inducer that functions by suppressing the glutathione peroxidase 4 (GPX4) activity. Macrophages were cultured at various concentrations of RSL-3 (0–800 nM) for 48 h, and then cell viability was evaluated. Increasing doses of RSL-3 led to a gradual decline in macrophage viability. At a concentration of 500 nM RSL-3, macrophage viability was significantly reduced (Fig. 1a). Ferroptosis-related factors, GPX4 and solute carrier family 7 member 11 (SLC7A11), are involved in restraining oxidative stress. Compared to the Ctrl group, both mRNA and GPX4 and SLC7A11 protein expression were remarkably reduced in the HG group (Fig. 1b, c, f). In addition, GSH content was reduced in the HG group, implying that the antioxidant capacity of macrophages was considerably diminished under HG conditions (Fig. 1g). Simultaneously, the MDA levels, a biomarker of ferroptosis, were remarkably increased in the HG group (Fig. 1h), indicating an increase in lipid peroxidation under HG conditions[25]. Iron metabolism-associated genes, including transferrin receptor (TFR-1) and ferroportin (FPN), were also affected by HG concentration in culture conditions. Specifically, our results showed that total iron concentration and TFR-1 expression levels were remarkably elevated, while the FPN level was markedly reduced in the HG group (Fig. 1d–f, i). Cumulatively, these observations suggest iron accumulation in macrophages exposed to HG – a pattern resembling that seen in macrophages treated with RSL-3, the ferroptosis inducer (Fig. 1b–i). Morphological analysis of the HG group further unveiled distinct

ferroptosis characteristics, including mitochondrial membrane disruption and alterations in mitochondrial cristae (Fig. 1j). No remarkable variations were observed among the Ctrl, DMSO, and mannitol groups (Fig. 1b–i), indicating that the hyperosmotic effect of HG on macrophages was ruled out.

3.2. Ferroptosis was observed in wounds of DM rats

To find out the potential involvement of ferroptosis in wound healing caused by diabetes, skin tissue samples from rats were subjected to immunohistochemical evaluations.The findings highlighted a notable reduction in the GPX4 and SLC7A11 protein expression in the DM (diabetic) group than the NC (non-diabetic control) group (Fig. 2a). Moreover, an enhanced staining intensity for the iron metabolism-associated gene, TFR-1, was observed in the DM group (Fig. 2a). Furthermore, qRT-PCR and western blotting showed a downregulation in the expression levels of GPX4, SLC7A11, and FPN, and upregulation in TFR-1 expression in DM rats compared to NC rats (Fig. 2b–f). When Compared to the NC group, MDA levels in the DM group were nearly 1.7 times higher, and the iron content was almost triple that of the control group (Fig. 2g and h). Further, a decline in GSH concentration was evident in the DM group (Fig. 2i). Importantly, the DM-associated ferroptosis indicators were substantially mitigated when the rats were reacted with the ferroptosis suppressor, Fer-1 (Fig. 2a–i).

3.3. Fer-1 protects against macrophage injury and ferroptosis induced by HG

Next, we delved into examining the protective role of Fer-1 against macrophage injury under HG conditions. Introducing Fer-1 (ranging from 0 to 1.4 μM) notably improved the viability of macrophages exposed to HG, with the most significant effect observed at a 1 μM concentration of Fer-1 (Fig. 3a). When Compared to the HG group, treatment with Fer-1 resulted in a remarkable upregulation in the GPX4, SLC7A11, and FPN expression as well as a downregulation in TFR-1 expression, at both levels of mRNA and protein (Fig. 3b–f). Additionally, Fer-1 administration culminated in reduced total iron and MDA concentrations, while amplifying the GSH content (Fig. 3h–j). Utilizing confocal fluorescence microscopy, we labeled the macrophages with DCFDA to discern the overall ROS levels. Utilizing confocal fluorescence microscopy, we labeled the macrophages with DCFDA to discern the overall ROS levels. Significantly, upon HG exposure, macrophages administered with Fer-1 manifested a subdued fluorescence intensity (Fig. 3g). Collectively, this data propounds that Fer-1 effectively mitigates macrophage injuries and ferroptosis instigated by hyperglycemia.

3.4. Anti-inflammatory effects of Fer-1 on HG-stimulated macrophages

To investigate the connection between ferroptosis and inflammation in HG-stimulated macrophages, the pro-inflammatory cytokine TNF-α and iNOS expression levels were evaluated in RAW264.7 cells. Initially, RAW264.7 cells were exposed to HG, followed by a 48-h treatment with either Fer-1 or DMSO. In the HG group, there was a notable upregulation in both mRNA and protein expressions of TNF-α and iNOS. Administering Fer-1 mitigated the HG-induced upregulation of TNF-α and iNOS expressions (Fig. 4a, b, e). Furthermore, we probed into the impact of Fer-1 on proliferative cytokines, specifically TGF-β and Arg-1. The data indicated that in HG-exposed RAW264.7 cells, Fer-1 treatment boosted both mRNA and protein expressions of TGF-β and Arg-1 (Fig. 4c–e).

3.5. Fer-1 promotes wound healing of DM rats

We further assessed the Fer-1 effects on the wound healing of STZ-induced DM rats. Fig. 5a shows representative images of wound areas in rats at days 0, 3, 7, 10, and 14 days after undergoing different treatments. In the NC group, the wound healing rate reached approximately 80 %, in stark contrast to the 42 % and 43 % observed in the DM and DM/VEH groups, respectively. In DM rats receiving Fer-1 treatment, a notable wound closure rate of 75 % was achieved by day 14 (Fig. 5b).

H&E and immunohistochemical staining were carried out on tissues at day 14. As depicted in Fig. 5c, persistent inflammatory cell penetration was observed in the DM and DM/VEH groups compared to the NC group. Treatment with Fer-1 decreased the inflammatory cellular penetration in DM rats (Fig. 5c).

Neovascularization is the basis of granulation tissue formation, contributing to wound healing. To assess wound healing quality, we conducted a semi-quantitative immunohistochemical analysis using CD31 as a indicator for neovascularization and angiogenesis in the injured tissue. Our results indicated that the number of CD31-positive cells in the DM group was lesser than the NC group. After Fer-1 treatment, there was a remarkable increase in CD31-positive cells in the DM rats (Fig. 5d and e).

Furthermore, the anti-inflammatory effects of Fer-1 on DM rats we assessed. Protein analysis showed increased TNF-α and iNOS expression levels in the DM rats, while administration of Fer-1 led to a decrease in their protein levels (Fig. 5f). We subsequently assessed the TGF-β and Arg-1 expression levels, pivotal players in the multiplicative phase of wound healing. Our findings revealed that the epidermal layer of wound tissues in DM rats had reduced TGF-β and Arg-1 protein levels compared to the NC rats. Nevertheless, the Fer-1 administration restored the TGF-β and Arg-1 expression levels in DM rats to levels that were nearly equivalent to those observed in NC rats (Fig. 5f). Collectively, these results indicate that Fer-1 promotes diabetic wound healing by alleviating inflammatory response and promoting neovascularization.

3.6. Fer-1 promotes Nrf2 activation in DM rats and HG-stimulated macrophages

Nrf2 takes place a pivotal role in redox homeostasis and inflammation. The fluorescence intensity of Nrf2 in wound tissues of DM

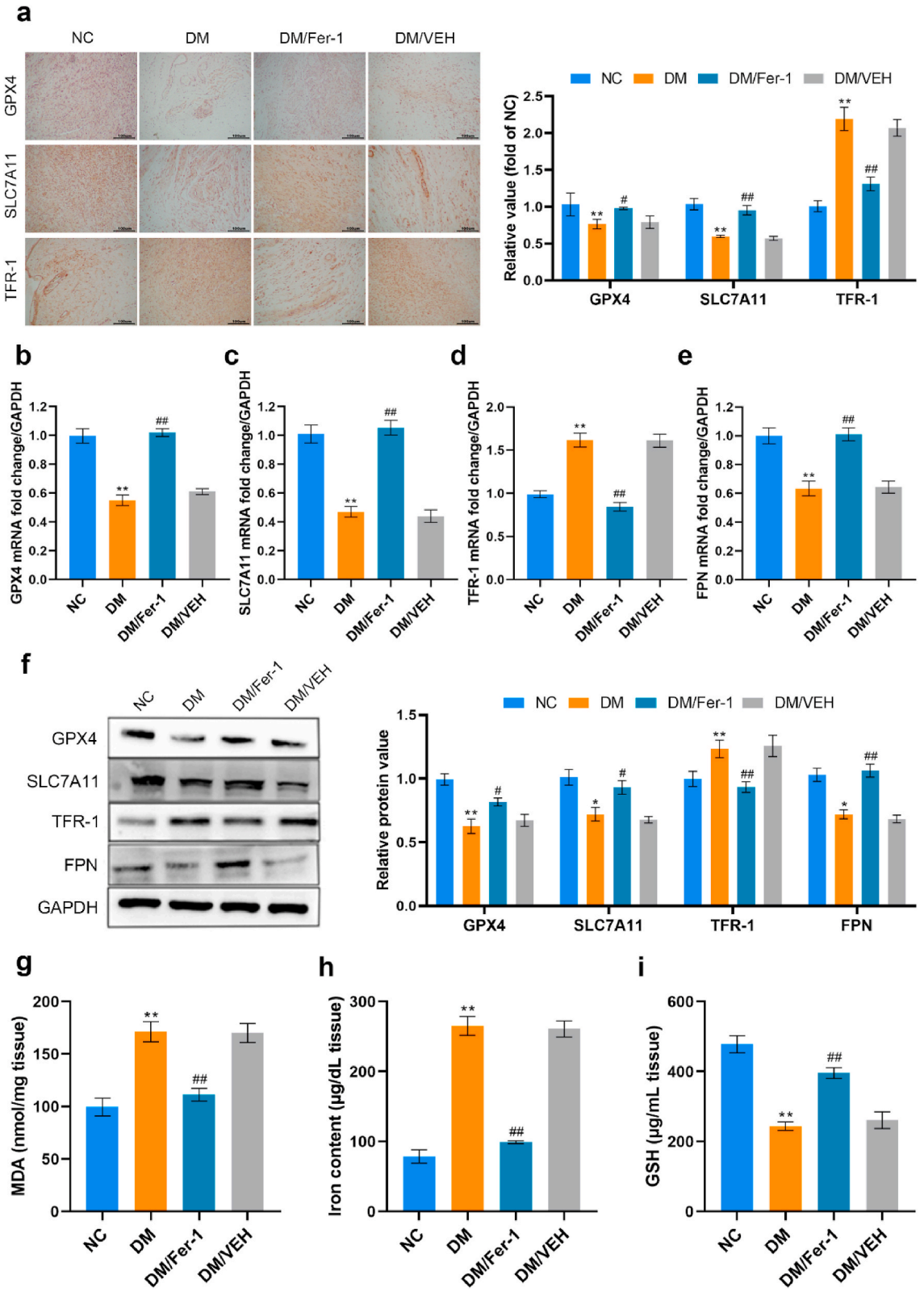

(caption on next page)

Fig. 2. Ferroptosis was observed in wounds of diabetes mellitus (DM) rats. (a) Immunohistochemical staining detected the GPX4, SLC7A11, and TFR-1 expression in rats. (b–f) The mRNA and protein expression of GPX4, SLC7A11, TFR-1, and FPN in wound tissues of rats. (g–i) The MDA,iron content,and GSH levels in wound tissue lysates of rats. Data expressed as mean ± SD. *p < 0.05 and **p < 0.01 vs. NC group; #p < 0.05 and ##p < 0.01 vs. DM group. The uncropped and full-size images for (Fig. 2f) this figure are provided in Supplementary Fig. S2.

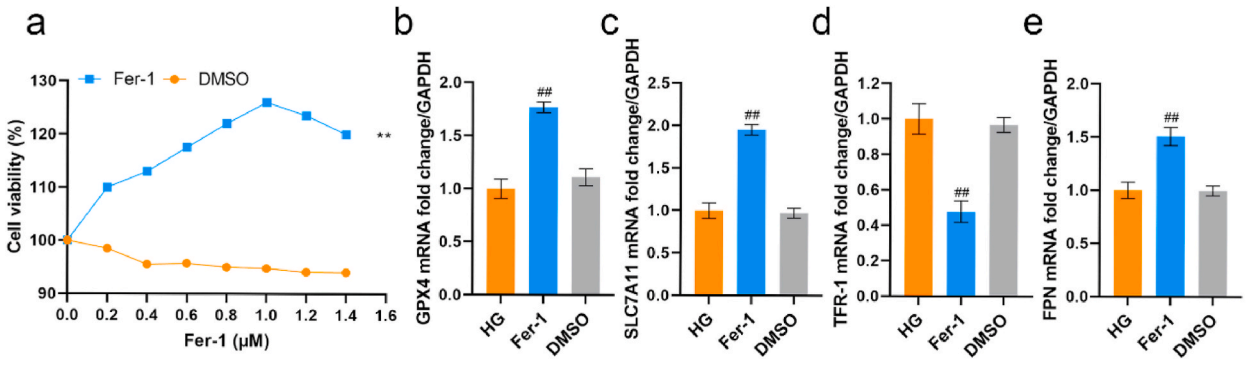

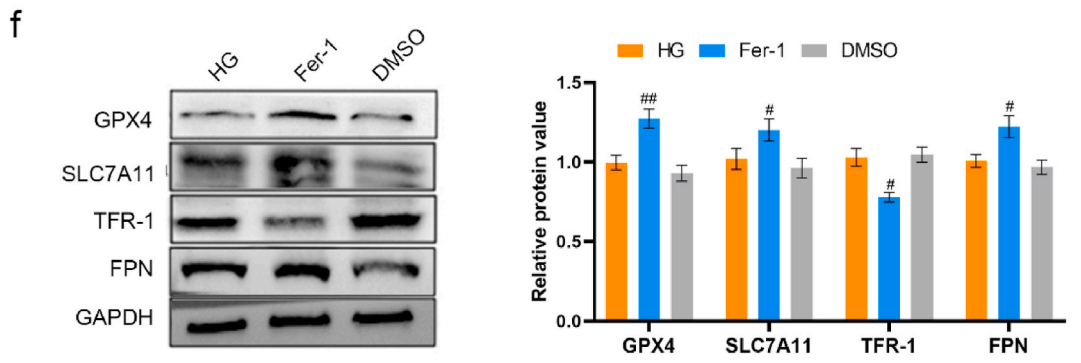

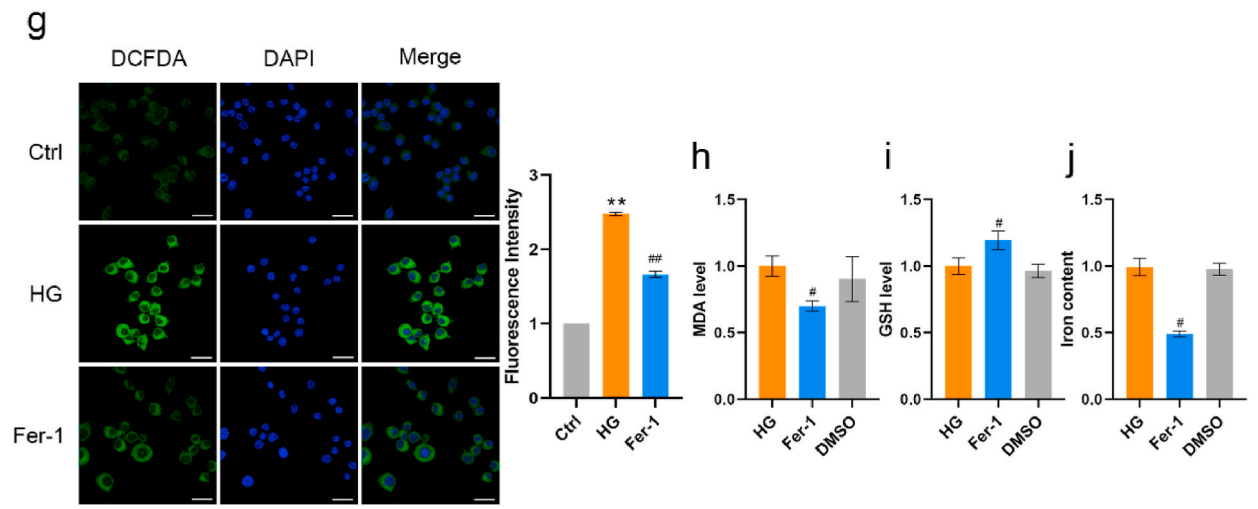

Fig. 3. Ferrostatin-1 (Fer-1) protects against macrophage injury and ferroptosis induced by HG. (a) The RAW264.7 cells viability was reacted with HG medium containing different doses of Fer-1 (0–1.4 μM). **p < 0.01 vs. DMSO group. (b–f) The mRNA and GPX4, SLC7A11, TFR-1, and FPN protein expression in cell lysates. (g) Fluorescence images of total ROS production in cells (Scale bar = 100 μm). (h–j) **p < 0.01 vs. Ctrl group, ##p < 0.01 vs. HG group. The MDA, GSH, and iron contents in cells. Values are presented as mean ± SD. #p < 0.05 and ##p < 0.01 vs. HG group. The uncropped and full-size images for (Fig. 3f) this figure are provided in Supplementary Fig. S3.

rats was remarkably lesser compared to that observed in NC rats. The fluorescence optical density of Nrf2 was elevated in DM rats after Fer-1 treatment (Fig. 6a). Both qRT-PCR and western blotting results consistently indicated altered Nrf2 expression in rats (Fig. 6b and c). Decreased Nrf2 mRNA (Fig. 6d) and protein (Fig. 6e) expression were evident in RAW264.7 cells upon HG stimulation. Treatment

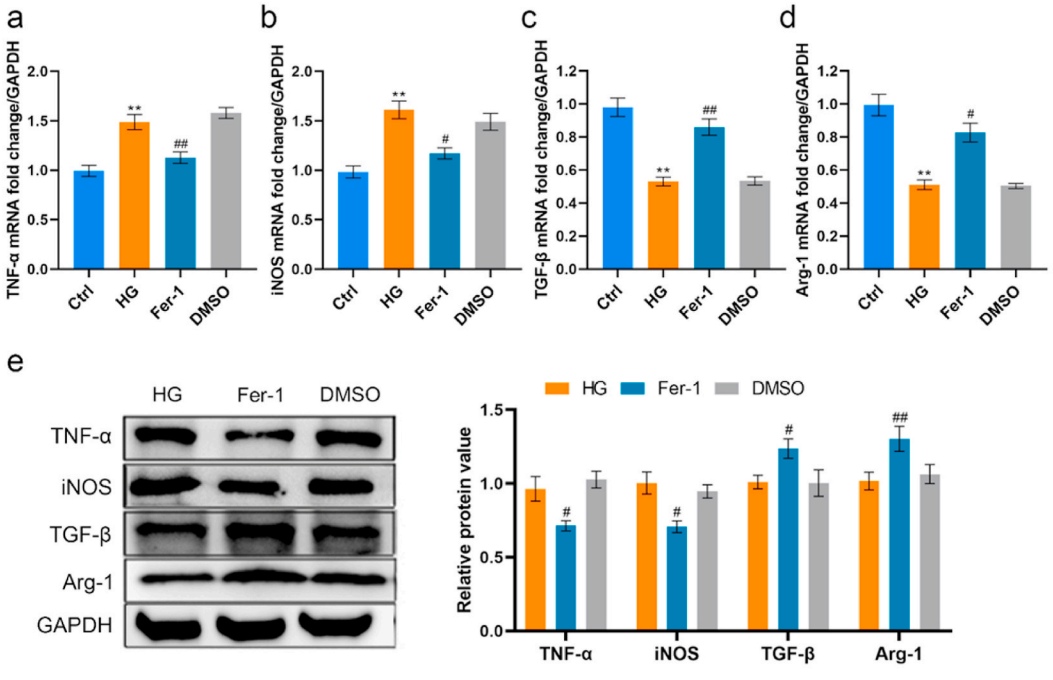

Fig. 4. Anti-inflammatory effects of Fer-1 on HG-stimulated macrophages. (a–d) qRT-PCR analysis of *TNF-α*, *iNOS*, *TGF-β*, and*Arg-1* in cell lysates. $^{**}p < 0.01$ vs.
Ctrl group. (e) Western blot analysis of TNF-α, iNOS, TGF-β, and Arg-1 protein levels in cell lysates. $\#p < 0.05$ and $\#\#p < 0.01$ vs. HG group. The uncropped and full-size images for (Fig. 4e) this figure are provided in Supplementary Fig. S4.

with Fer-1 enhanced Nrf2 expression in both *in vivo* and *in vitro* diabetes models.

4. Discussion

In this study, we found that ferroptosis is evident in HG-stimulated macrophages and DM model rats, depicted by increased iron content, lipid peroxidation, and oxidative stress. The results indicate that ferroptosis may contribute to the pathogenesis and progression of diabetic wounds. In addition, DM rats exhibited sustained inflammation, as evidenced by increased inflammatory cytokines TNF-α and iNOS. We found that administering Fer-1, a ferroptosis inhibitor, effectively mitigates diabetes-associated ferroptosis, reduces inflammation, fosters cell proliferation and neovascularization, and expedites the healing of diabetic wounds.Moreover, our data indicate that Fer-1 might mediate its anti-ferroptotic and anti-inflammatory actions by activating Nrf2.

Iron, an essential trace element, takes place a significant part in cellular survival and metabolism. It takes place a different essential processes such as DNA synthesis, erythropoiesis, mitochondrial biosynthesis, metabolism of energy and transport of oxygen. Excessive intracellular iron produces ROS via the Fenton reaction, leading to macrophage dysfunction. This dysfunction impairs wound healing and adversely affects ulcer healing [26]. Moreover, the presence of residual iron in the wound bed promotes the production of TNF-α, which exacerbates the inflammatory response[27]. In a previous mouse model of overload of iron, the iron chelator, deferasirox, was shown to enhance wound healing[28]. These studies suggest that iron overload harms the occurrence and progression of diabetic wound healing. However, the basic mechanism remains elusive. Ferroptosis is a new perspective on the pathogenesis involving excess iron in disease. Here, we proposed that ferroptosis exacerbates the pathological damage in diabetic wounds, leading to delayed healing. TFR-1 and FPN are crucial transport proteins in the iron homeostasis regulation [29]. Transferrin binds to free iron and into cells via the intermediation of TFR-1. Therefore, TFR-1 is an important regulator of iron-mediated cellular death by controlling the intracellular available iron[30,31]. Intracellularly, iron is stored in the form of ferritin or in labile iron pools, with its export linked to FPN expression. FPN is the only mammalian exporter of iron and a decrease in FPN expression leads to elevated intracellular iron levels [32]. Our study observed a pronounced upregulation of TFR-1 expression and a notable downregulation of FPN expression in both *in vivo* and *in vitro* diabetic wound healing models. This finding implies that ferroptosis occurs in DM and may takes place a role in wound healing caused by diabetes.

Wound healing caused by Diabetes is compromised as a result of elevated ROS levels and decreased activity of antioxidant enzymes in injured tissues[33]. Persistent oxidative stress and the lipid peroxides accumulation contribute to the delay in wound healing. ROS takes place an important part in the ferroptosis initiation, and our study showed elevated levels in HG-stimulated macrophages. In addition, GPX4 is a basic ferroptosis regulator owing to its distinct antioxidant activity, which enables it to eliminate harmful byproducts of iron-dependent lipid peroxidation, thereby preventing damage of cell membrane[34]. Downregulation of GPX4 leads to

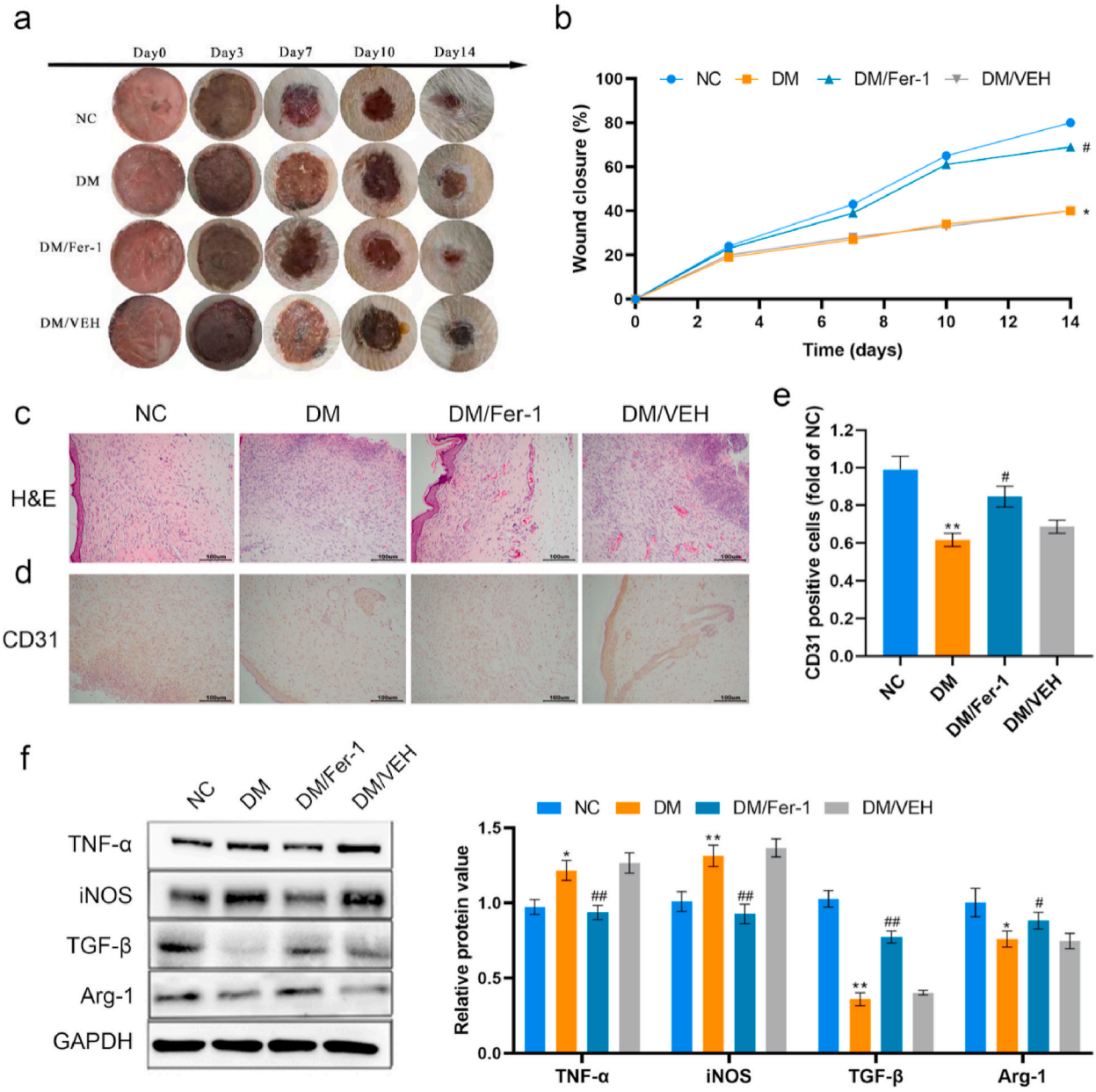

Fig. 5. Fer-1 promotes wound healing in DM rats. (a–b) Representative wound images and corresponding wound healing rate on days 0, 3, 7, 10, and 14. (c) H&E staining (Scale bar = 100 μm). (d–e) Immunohistochemical staining and corresponding quantification of CD31-positive cells in wounds of rats (Scale bar = 100 μm). (f) Representative western blots and quantification of TNF-α, iNOS, TGF-β, and Arg-1 protein levels in wounds of rats.Data expressed as mean ± SD. *p < 0.05 and **p < 0.01 vs. NC group; #p < 0.05 and ##p < 0.01 vs. DM group. The uncropped and full-size images for (Fig. 5f) this figure are provided in Supplementary Fig. S5.

substantial accumulation of the lethal lipid peroxide MDA, leading to ferroptosis [35].SLC7A11, a crucial component of the cystine-glutamate antiporter (XC^-) system[36], is responsible for introducing cysteine into cells[37], where it is further reduced to cysteine. Cysteine is converted to GSH in cells by the addition of glutamate and glycine. GSH serves as both a cofactor and substrate of GPX4 and is necessary for the lipid repair function of the enzyme. GPX4 can convert potentially poisonous lipid peroxides into nontoxic lipid alcohols, thus preventing the lipid ROS accumulation[35]. Consequently, the downregulation of SLC7A11 hinders the intracellular import of cysteine, leading to a decrease in GSH synthesis and GPX4 activity, as well as the accumulation of lipid hydroperoxides. Our findings indicate a remarkable reduction in SLC7A11 and GPX4 expression in both HG-stimulated macrophages and in the wounds of DM rats. Additionally, we observed reduced GSH and increased MDA levels in HG-stimulated macrophages and the wounds of DM rats. These results further recommended that ferroptosis is involved in the pathogenesis of wound healing caused by

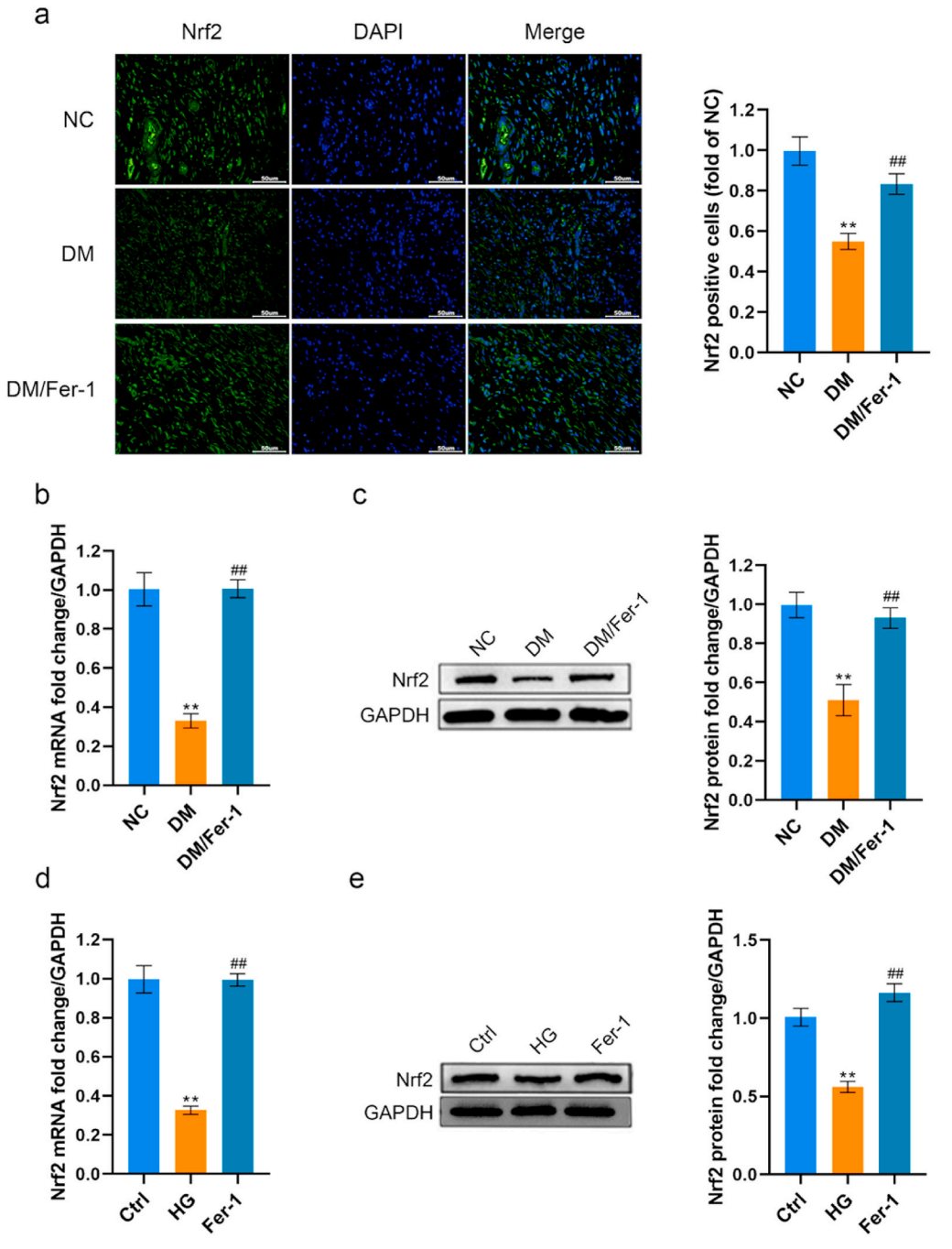

Fig. 6. Fer-1 promotes Nrf2 activation in DM rats and HG-stimulated macrophages. (a) Immunofluorescence evaluation using Nrf2 antibody in wound tissue sections of rats (Scale bar = 50 μm). (b–c) Relative mRNA and protein expression of Nrf2 in wound tissues lysates of rats. (d–e) The Nrf2 mRNA and protein expression in RAW264.7 cell lysates. Values are indicated as mean ± SD.**$p < 0.01$ vs. NC or Ctrl group; ##$p < 0.01$ vs. HG or DM group. The uncropped and full-size images for (Fig. 6c–e) this figure are provided in Supplementary Fig. S6.

diabetes.

Chronic diabetic wounds are related with inflammation, as evidenced by increased pro-inflammatory cytokines and proteases levels, also impaired growth factors expression [38,39]. Excess ROS perpetuates the inflammatory response in diabetic wound tissues [8].Ferroptosis induced by cellular lipid peroxidation can trigger and amplify inflammatory responses[36,40–42]. We assessed the alterations in inflammatory markers in HG-stimulated macrophages and STZ-induced DM rats, revealing an upregulation of inflammatory cytokines (TNF-α and iNOS). H&E staining further highlighted pronounced inflammatory infiltration in the wound tissues of

DM rats. Treatment with Fer-1 effectively mitigated inflammation by reducing inflammatory cellular infiltration and pro-inflammatory cytokines. Angiogenesis is crucial at all stages of wound healing. Blood vessels provide progenitor cells, nutrients, and oxygen necessary to sustain cell multiplication and the remodeling of wound sites [43]. Therefore, impaired angiogenesis is one of the most important factors delaying wound healing caused by diabetes. To determine the level of tissue angiogenesis, we employed immunohistochemical staining with CD31, a marker for endothelial cells. CD31-positive cells were found to be most prevalent at the wound site of DM rats treated with Fer-1. TGF-β facilitates the granulation tissue formation and wound angiogenesis by modulating fibroblast multiplication and differentiation [44–46]. In diabetes-induced delayed wound healing, the expression of TGF-β is downregulated [47], leading to increased infiltration of inflammatory cells and delayed wound healing [48]. Our findings indicate that administration of Fer-1 increased TGF-β expression in the wounds of DM rats. Collectively, these findings underscore the capacity of Fer-1 to diminish inflammation and enhance angiogenesis, facilitating diabetic wound healing.

In addition, Fer-1 reportedly enhances the differentiation of brain microglia into M2 phenotype and reduces the inflammatory response after cerebral hemorrhage[49]. The phenotypic transformation of macrophages takes place an essential part in the diabetic wound-healing process [1]. Classically activated, or M1-like macrophages, possess microbicidal properties and secrete pro-inflammatory cytokines, namely TNF-α, interleukin (IL)-1β, IL-6 and iNOS [50]. In contrast, alternately stimulated or M2-like macrophages produce Arg-1, IL-10, TGF-β, and insulin-like growth factor-1 (IGF-1) that promotes inflammation and wound regeneration [51]. The macrophage transition from M1 to M2 phenotype is considered a pre-requisite for the shift from the inflammatory to the multiplicative phase of wound healing[52]. Our study determined that Fer-1 enhances the expression of M2-associated factors, namely Arg-1 and TGF-β, in HG-stimulated macrophages and DM rats. Despite the positive effect of Fer-1 on promoting the phenotypic transformation of macrophages in DM, the exact mechanism by which Fer-1 induces this transformation requires further investigation.

Given its pivotal role in the cellular stress response, Nrf2 has surfaced as a potential therapeutic target for conditions ranging from neurodegenerative diseases and cancers to diabetes, liver cirrhosis, and chronic wound healing. Prolonged hyperglycemia fosters an environment conducive to ROS accumulation, which subsequently impairs wound healing in diabetic patients. Our investigations revealed a surge in ROS production within HG-stimulated macrophages. Nrf2, detected as a basic controller of skin inflammation, can thwart inflammation by inhibiting the pro-inflammatory cytokines transcription [53–55]. A previous study has demonstrated that Nrf2 stimulation accelerates impaired diabetic wound healing by oxidative stress amelioration and inflammation[56]. Both HG-stimulated macrophages and DM rats exhibited diminished Nrf2 expression. Interestingly, our results showed that Nrf2 expression was increased in HG-stimulated macrophages and DM rats following Fer-1 treatment. Previous research has shown that Fer-1 alleviates damage from oxidative stress, diminishes iron accumulation, betters mitochondrial morphology, and eases renal pathological damage in diabetic mice[3]. Given that Nrf2 orchestrates the enhancement of oxidative responses, there seems to be a regulatory interplay between Fer-1 and Nrf2. Notably, Xie et al. reported that Fer-1 augments Nrf2 expression, thereby mitigating liver damage resulting from sepsis[17]. In line with this, we observed elevated Nrf2 expression in DM rats, which was associated with enhanced wound healing after Fer-1 treatment. These observations imply that the promotion of diabetic wound healing by Fer-1 may be mediated via the activation of Nrf2.

5. Conclusion

This study highlights the major part of cellular ferroptosis and inflammation in the impaired wound-healing process of diabetes. Fer-1 can mitigate ferroptosis and inflammation, potentially through Nrf2 activation, thereby promoting wound healing in DM. A deeper exploration is warranted to elucidate the mechanisms by which Fer-1 influences diabetic wound healing. Specifically, investigating the role of ferroptosis and Nrf2 activation can be performed using techniques such as *Nrf2* knockdown or overexpression. Insights from this study furnish a compelling argument for considering ferroptosis inhibitors as potential therapeutic agents in diabetic wound healing.

Availability of data and materials

The data used to support this study are available from the corresponding author upon request.

Ethical statement

All the animal experiments have complied with the guidelines of the Tianjin Medical Experimental Animal Care, and animal protocols were approved by the Institutional Animal Care and Use Committee of Yi Shengyuan Gene Technology (Tianjin) Co., Ltd. (approval No. YSY-DWLL-2022081).

Funding statement

This work was supported by the National Natural Science Foundation of China (32171339), the Joint Fund for Innovation and Development of Shandong Provincial Natural Science Foundation (ZR2022LZY028), Taishan Scholars Program of Shandong Province (tstp20221161), the Inner Mongolia people's Hospital Foundation (2021YN21), Clinical Need Oriented Basic Research Project of Inner Mongolia Academy of Medical Sciences (2023GLLH0098) and Tianjin Key Medical Discipline (Specialty) Construction Project (TJYXZDXK-032A).

CRediT authorship contribution statement

Tongcai Wang: Writing – review & editing, Writing – original draft. **Yin Zheng:** Methodology, Investigation. **Jun Zhang:** Data curation, Conceptualization. **Zhongming Wu:** Validation, Supervision.

Declaration of competing interest

The authors declare the following financial interests/personal relationships which may be considered as potential competing interests:Zhongming Wu reports financial support was provided by Shandong Institute of Endocrine and Metabolic Diseases. Zhongming Wu reports a relationship with Tianjin Medical University that includes: employment and funding grants. If there are other authors, they declare that they have no known competing financial interests or personal relationships that could have appeared to influence the work reported in this paper.

Appendix A. Supplementary data

Supplementary data to this article can be found online at https://doi.org/10.1016/j.heliyon.2024.e37477.

References

[1] S. Patel, S. Srivastava, M.R. Singh, et al., Mechanistic insight into diabetic wounds: pathogenesis, molecular targets and treatment strategies to pace wound healing, Biomed. Pharmacother. 112 (2019) 108615. https://doi:10.1016/j.biopha.2019.108615.
[2] W.J. Jeffcoate, K.G. Harding, Diabetic foot ulcers, Lancet 361 (9368) (2003) 1545–1551. https://doi:10.1016/S0140-6736(03)13169-8.
[3] S. Li, Y. Li, Z. Wu, et al., Diabetic ferroptosis plays an important role in triggering on inflammation in diabetic wound, Am. J. Physiol. Endocrinol. Metab. 321 (4) (2021). E509-e20, https://doi:10.1152/ajpendo.00042.2021.
[4] J.B. Hansen, I.W. Moen, T. Mandrup-Poulsen, Iron: the hard player in diabetes pathophysiology, Acta Physiol. 210 (4) (2014) 717–732. https://doi:10.1111/apha.12256.
[5] J.M. FernáNDEZ-Real, A. LóPEZ-Bermejo, W. Ricart, Cross-talk between iron metabolism and diabetes, Diabetes 51 (8) (2002) 2348–2354. https://doi:10.2337/diabetes.51.8.2348.
[6] M. SchäFER, S. Werner, Oxidative stress in normal and impaired wound repair, Pharmacol. Res. 58 (2) (2008) 165–171. https://doi:10.1016/j.phrs.2008.06.004.
[7] M. Wlaschek, K. Scharffetter-Kochanek, Oxidative stress in chronic venous leg ulcers, Wound Repair Regen. 13 (5) (2005) 452–461. https://doi:10.1111/j.1067-1927.2005.00065.x.
[8] N. Bryan, H. Ahswin, N. Smart, et al., Reactive oxygen species (ROS)–a family of fate deciding molecules pivotal in constructive inflammation and wound healing, Eur. Cell. Mater. 24 (2012) 249–265. https://doi:10.22203/ecm.v024a18.
[9] C.C. Smith, D.M. Yellon, Necroptosis, necrostatins and tissue injury, J. Cell Mol. Med. 15 (9) (2011) 1797–1806. https://doi:10.1111/j.1582-4934.2011.01341.x.
[10] J.D. Hayes, A.T. Dinkova-Kostova, The Nrf2 regulatory network provides an interface between redox and intermediary metabolism, Trends Biochem. Sci. 39 (4) (2014) 199–218. https://doi:10.1016/j.tibs.2014.02.002.
[11] M.J. Kerins, A. Ooi, The roles of NRF2 in modulating cellular iron homeostasis, Antioxid Redox Signal 29 (17) (2018) 1756–1773. https://doi:10.1089/ars.2017.7176.
[12] S.T. Li, Q. Dai, S.X. Zhang, et al., Ulinastatin attenuates LPS-induced inflammation in mouse macrophage RAW264.7 cells by inhibiting the JNK/NF-κB signaling pathway and activating the PI3K/Akt/Nrf2 pathway, Acta Pharmacol. Sin. 39 (8) (2018) 1294–1304. https://doi:10.1038/aps.2017.143.
[13] Y. Shou, L. Yang, Y. Yang, et al., Inhibition of keratinocyte ferroptosis suppresses psoriatic inflammation, Cell Death Dis. 12 (11) (2021) 1009. https://doi:10.1038/s41419-021-04284-5.
[14] N. Harada, M. Kanayama, A. Maruyama, et al., Nrf2 regulates ferroportin 1-mediated iron efflux and counteracts lipopolysaccharide-induced ferroportin 1 mRNA suppression in macrophages, Arch. Biochem. Biophys. 508 (1) (2011) 101–109. https://doi:10.1016/j.abb.2011.02.001.
[15] W. Yu, W. Liu, D. Xie, et al., High level of uric acid promotes atherosclerosis by targeting NRF2-mediated autophagy dysfunction and ferroptosis, Oxid. Med. Cell. Longev. 2022 (2022) 9304383. https://doi:10.1155/2022/9304383.
[16] Y. Chen, W. He, H. Wei, et al., Srs11-92, a ferrostatin-1 analog, improves oxidative stress and neuroinflammation via Nrf2 signal following cerebral ischemia/reperfusion injury, CNS Neurosci. Ther. 29 (6) (2023) 1667–1677. https://doi:10.1111/cns.14130.
[17] L. Xie, C. Zhou, Y. Wu, et al., Wenqingyin suppresses ferroptosis in the pathogenesis of sepsis-induced liver injury by activating the Nrf2-mediated signaling pathway, Phytomedicine 114 (2023) 154748. https://doi:10.1016/j.phymed.2023.154748.
[18] J. Duan, M. Yang, Y. Liu, et al., Curcumin protects islet beta cells from streptozotocin-induced type 2 diabetes mellitus injury via its antioxidative effects, Endokrynol. Pol. 73 (6) (2022) 942–946. https://doi:10.5603/EP.a2022.0070.
[19] H.Z. Asfour, N.A. Alhakamy, O.A.A. Ahmed, et al., Enhanced healing efficacy of an optimized gabapentin-melittin nanoconjugate gel-loaded formulation in excised wounds of diabetic rats, Drug Deliv. 29 (1) (2022) 1892–1902. https://doi:10.1080/10717544.2022.2086943.
[20] Y. Ning, Y. Gong, T. Zheng, et al., Lingguizhugan decoction targets intestinal microbiota and metabolites to reduce insulin resistance in high-fat diet rats, Diabetes Metab Syndr Obes 15 (2022) 2427–2442. https://doi:10.2147/DMSO.S370492.
[21] D S, T.A.M. Andrade, G.F. Caetano, et al., Experimental models and methods for cutaneous wound healing assessment, Int. J. Exp. Pathol. 101 (1–2) (2020) 21–37, 10.1111/iep.12346.MARTINA.Theuseofantioxidantsinhealing . Dermatol Surg, 1996, 22(2): 156-60, https://doi:10.1111/j.1524-4725.1996.tb00499.x.
[22] D.S. Masson-Meyers, T.A.M. Andrade, G.F. Caetano, et al., Experimental models and methods for cutaneous wound healing assessment, Int. J. Exp. Pathol. 101 (1–2) (2020) 21–37. https://doi:10.1111/iep.12346.
[23] X. Fan, M. Xu, Q. Ren, et al., Downregulation of fatty acid binding protein 4 alleviates lipid peroxidation and oxidative stress in diabetic retinopathy by regulating peroxisome proliferator-activated receptor γ-mediated ferroptosis, Bioengineered 13 (4) (2022) 10540–10551. https://doi:10.1080/21655979.2022.2062533.
[24] S.Y. Kim, M.G. Nair, Macrophages in wound healing: activation and plasticity, Immunol. Cell Biol. 97 (3) (2019) 258–267. https://doi:10.1111/imcb.12236.
[25] L.H. Xie, N. Fefelova, S.H. Pamarthi, J.K. Gwathmey, Molecular mechanisms of ferroptosis and relevance to cardiovascular disease, Cells 11 (17) (2022 Sep 1) 2726.
[26] Y. Zhou, K.T. Que, Z. Zhang, et al., Iron overloaded polarizes macrophage to proinflammation phenotype through ROS/acetyl-p53 pathway, Cancer Med. 7 (8) (2018) 4012–4022. https://doi:10.1002/cam4.1670.

[27] A. Kroner, A.D. Greenhalgh, J.G. Zarruk, et al., TNF and increased intracellular iron alter macrophage polarization to a detrimental M1 phenotype in the injured spinal cord, Neuron 83 (5) (2014) 1098–1116. https://doi:10.1016/j.neuron.2014.07.027.
[28] A. Sindrilaru, T. Peters, S. Wieschalka, et al., An unrestrained proinflammatory M1 macrophage population induced by iron impairs wound healing in humans and mice, J. Clin. Invest. 121 (3) (2011) 985–997. https://doi:10.1172/JCI44490.
[29] Q. Liu, J. Wu, X. Zhang, et al., Iron homeostasis and disorders revisited in the sepsis, Free Radic. Biol. Med. 165 (2021) 1–13. https://doi:10.1016/j.freeradbiomed.2021.01.025.
[30] G. Corna, L. Campana, E. Pignatti, et al., Polarization dictates iron handling by inflammatory and alternatively activated macrophages, Haematologica 95 (11) (2010) 1814–1822. https://doi:10.3324/haematol.2010.023879.
[31] M. Gao, P. Monian, N. Quadri, et al., Glutaminolysis and transferrin regulate ferroptosis, Mol Cell 59 (2) (2015) 298–308. https://doi:10.1016/j.molcel.2015.06.011.
[32] W.D. Bao, P. Pang, X.T. Zhou, et al., Loss of ferroportin induces memory impairment by promoting ferroptosis in Alzheimer's disease, Cell Death Differ. 28 (5) (2021) 1548–1562. https://doi:10.1038/s41418-020-00685-9.
[33] W.N. Hozzein, G. Badr, B.M. Badr, et al., Bee venom improves diabetic wound healing by protecting functional macrophages from apoptosis and enhancing Nrf2, Ang-1 and Tie-2 signaling, Mol. Immunol. 103 (2018) 322–335. https://doi:10.1016/j.molimm.2018.10.016.
[34] T. Luo, Q. Zheng, L. Shao, et al., Intracellular delivery of glutathione peroxidase degrader induces ferroptosis in vivo, Angew Chem. Int. Ed. Engl. 61 (39) (2022) e202206277. https://doi:10.1002/anie.202206277.
[35] H. Feng, B.R. Stockwell, Unsolved mysteries: how does lipid peroxidation cause ferroptosis? PLoS Biol. 16 (5) (2018) e2006203. https://doi:10.1371/journal.pbio.2006203.
[36] L. Iang, N. Kon, T. Li, et al., Ferroptosis as a p53-mediated activity during tumour suppression, Nature 520 (7545) (2015) 57–62. https://doi:10.1038/nature14344.
[37] S.J. Dixon, K.M. Lemberg, M.R. Lamprecht, et al., Ferroptosis: an iron-dependent form of nonapoptotic cell death, Cell 149 (5) (2012) 1060–1072. https://doi:10.1016/j.cell.2012.03.042.
[38] R.E. Mirza, M.M. Fang, E.M. Weinheimer-Haus, et al., Sustained inflammasome activity in macrophages impairs wound healing in type 2 diabetic humans and mice, Diabetes 63 (3) (2014) 1103–1114. https://doi:10.2337/db13-0927.
[39] S. Akita, Wound repair and regeneration: mechanisms, signaling, Int. J. Mol. Sci. 20 (24) (2019) 6328. https://doi:10.3390/ijms20246328.
[40] A.E. Boniakowski, A.S. Kimball, B.N. Jacobs, et al., Macrophage-mediated inflammation in normal and diabetic wound healing, J. Immunol. 199 (1) (2017) 17–24. https://doi:10.4049/jimmunol.1700223.
[41] X. Chen, X. Li, X. Xu, et al., Ferroptosis and cardiovascular disease: role of free radical-induced lipid peroxidation, Free Radic. Res. 55 (4) (2021) 405–415. https://doi:10.1080/10715762.2021.1876856.
[42] S. David, F. Ryan, P. Jhelum, et al., Ferroptosis in neurological disease, Neuroscientist 29 (5) (2023) 591–615. https://doi:10.1177/10738584221100183.
[43] S. Tsurusaki, Y. Tsuchiya, T. Koumura, et al., Hepatic ferroptosis plays an important role as the trigger for initiating inflammation in nonalcoholic steatohepatitis, Cell Death Dis. 10 (6) (2019) 449. https://doi:10.1038/s41419-019-1678-y.
[44] R.D. Galiano, O.M. Tepper, C.R. Pelo, et al., Topical vascular endothelial growth factor accelerates diabetic wound healing through increased angiogenesis and by mobilizing and recruiting bone marrow-derived cells, Am. J. Pathol. 164 (6) (2004) 1935–1947. https://doi:10.1016/S0002-9440(10)63754-6.
[45] I. Pastar, O. Stojadinovic, A. Krzyzanowska, et al., Attenuation of the transforming growth factor beta-signaling pathway in chronic venous ulcers, Mol Med 16 (3–4) (2010) 92–101. https://doi:10.2119/molmed.2009.00149.
[46] M.K. Lichtman, M. Otero-Vinas, V. Falanga, Transforming growth factor beta (TGF-β) isoforms in wound healing and fibrosis, Wound Repair Regen. 24 (2) (2016) 215–222. https://doi:10.1111/wrr.12398.
[47] Y. Yuan, J. Gao, L. Liu, et al., Role of adipose-derived stem cells in enhancing angiogenesis early after aspirated fat transplantation: induction or differentiation? Cell Biol. Int. 37 (6) (2013) 547–550. https://doi:10.1002/cbin.10068.
[48] M.S. Bitar, Z.N. Labbad, Transforming growth factor-beta and insulin-like growth factor-I in relation to diabetes-induced impairment of wound healing, J. Surg. Res. 61 (1) (1996) 113–119. https://doi:10.1006/jsre.1996.0090.
[49] L. Huang, Y. Zhang, L. Zhao, et al., Ferrostatin-1 polarizes microglial cells toward M2 phenotype to alleviate inflammation after intracerebral hemorrhage, Neurocrit Care 36 (3) (2022) 942–954. https://doi:10.1007/s12028-021-01401-2.
[50] M.L. Novak, T.J. Koh, Phenotypic transitions of macrophages orchestrate tissue repair, Am. J. Pathol. 183 (5) (2013) 1352–1363. https://doi:10.1016/j.ajpath.2013.06.034.
[51] G.T. Bardi, M.A. Smith, J.L. Hood, Melanoma exosomes promote mixed M1 and M2 macrophage polarization, Cytokine 105 (2018) 63–72. https://doi:10.1016/j.cyto.2018.02.002.
[52] T.L. Fernandes, A.H. Gomoll, C. Lattermann, et al., Macrophage: a potential target on cartilage regeneration, Front. Immunol. 11 (2020) 111. https://doi:10.3389/fimmu.2020.00111.
[53] S. Braun, C. Hanselmann, M.G. Gassmann, et al., Nrf2 transcription factor, a novel target of keratinocyte growth factor action which regulates gene expression and inflammation in the healing skin wound, Mol. Cell Biol. 22 (15) (2002) 5492–5505. https://doi:10.1128/MCB.22.15.5492-5505.2002.
[54] E.H. Kobayashi, T. Suzuki, R. Funayama, et al., Nrf2 suppresses macrophage inflammatory response by blocking proinflammatory cytokine transcription, Nat. Commun. 7 (2016) 11624. https://doi:10.1038/ncomms11624.
[55] Y. Cui, Z. Zhang, X. Zhou, et al., Microglia and macrophage exhibit attenuated inflammatory response and ferroptosis resistance after RSL3 stimulation via increasing Nrf2 expression, J. Neuroinflammation 18 (1) (2021) 249. https://doi:10.1186/s12974-021-02231-x.
[56] M. Li, H. Yu, H. Pan, et al., Nrf2 suppression delays diabetic wound healing through sustained oxidative stress and inflammation, Front. Pharmacol. 10 (2019) 1099. https://doi:10.3389/fphar.2019.01099.